

# Vacuole-inducing compounds that disrupt endolysosomal trafficking stimulate production of exosomes by glioblastoma cells

Zehui Li<sup>1</sup> · Nneka E. Mbah<sup>1</sup> · William A. Maltese<sup>1</sup> 

Received: 20 February 2017 / Accepted: 26 July 2017  
© Springer Science+Business Media, LLC 2017

**Abstract** Exosomes are produced from mammalian cells when multivesicular endosomes fuse with the plasma membrane, releasing their intraluminal vesicles. In this study we assessed the effects of MOPIPP, a novel indole-based chalcone, and vacuolin-1, a distinct triazine-based compound, on exosome production in cultured glioblastoma and 293T cells. Both compounds promote vacuolization of late endosome compartments and interfere with trafficking of late endosomes to lysosomes, without significant cytotoxicity. The results show that vacuolated cells treated with these compounds release exosomes with morphologies similar to untreated controls. However, both compounds trigger multi-fold increases in release of exosome marker proteins (e.g., CD63, Alix) in exosome fractions collected from equivalent numbers of cells. Despite the marked increase in exosome production, the profiles of selected miRNA cargoes carried by the exosomes were generally similar in cells treated with the compounds. Insofar as MOPIPP and vacuolin-1 seem able to increase the overall yield of exosomes from cultured cells, they might be useful for efforts to develop exosome-based therapeutics.

**Keywords** Exosome · Vacuoles · Endosomes · Glioblastoma · Chalcones · Vacuolin

## Introduction

Exosomes are vesicles with diameters in the range of 30–120 nm, which are released from many types of cells [1, 2]. The roles of exosomes in cancer have attracted particular interest because of the possibility that molecules carried by these vesicles may serve as biomarkers to monitor tumor occurrence and progression [3, 4]. Mounting evidence suggests that exosomes also play important roles in mediating intercellular communication within the tumor microenvironment [5, 6] and promoting cancer invasion and metastasis [7]. Finally, exosomes have attracted considerable attention as potential nanocarriers for delivery of drugs and other therapeutic cargoes, such as miRNAs [8, 9].

Exosomes originate as intraluminal vesicles (ILVs) within multivesicular late endosomes (MVEs). The vesicles are released into the extracellular environment upon fusion of MVEs with the plasma membrane [10, 11]. MVEs are commonly viewed as occupying an intermediate position between early endosomes and lysosomes in the endolysosomal degradative pathway of eukaryotic cells [12]. Several distinct multiprotein ESCRTs (endosomal sorting complexes required for transport) function in MVE biogenesis [13]. Proteins displaying monoubiquitin signals interact with the ESCRTs and are sorted into the intraluminal vesicles, which are ultimately degraded when the MVEs merge with lysosomes. While exosomes contain proteins typically found in ILVs, there is some evidence that they may be derived from functionally distinct subpopulations of MVEs that are routed to the plasma membrane instead of the lysosomes [14]. The mechanisms that control the trafficking of MVEs to the cell surface and the release of exosomes are not well understood. Nevertheless, several common factors appear to influence this process, including ceramide levels [15], intracellular calcium [16],

---

✉ William A. Maltese  
william.maltese@utoledo.edu

<sup>1</sup> Department of Biochemistry and Cancer Biology, University of Toledo College of Medicine and Life Sciences, 3000 Arlington Avenue, Toledo, OH 43617, USA

microenvironmental pH [17], and specific Rab GTPases [18–20].

Despite intense interest in the potential diagnostic and therapeutic applications of exosomes, small molecules that can either inhibit or stimulate exosome production without affecting cell growth or viability are lacking. Many compounds that perturb endolysosomal vesicle trafficking and induce vacuolization of late endosomal compartments have been identified [21, 22]. However, little is known about the possible effects of such compounds on exosome biogenesis because many of them are cytotoxic. We have been working with a series of synthetic indole-based chalcones with the goal of discovering new therapeutic agents that trigger non-apoptotic cell death in cancer cells. Our lead compound, 3-(5-methoxy-2-methyl-1*H*-indol-3-yl)-1-(4-pyridinyl)-2-propene-1-one (abbreviated MOMIPP), induces a form of cell death termed ‘methuosis,’ which is characterized by the accumulation of large vacuoles derived from macropinosomes and late endosomes [22, 23]. In the course of performing structure–activity studies with MOMIPP analogs, we identified several derivatives that induce endosomal vacuolization but, surprisingly, do not trigger growth arrest or cell death [24, 25]. One of these non-lethal compounds is abbreviated as MOIIPP, since it is identical to MOMIPP, except for the presence of a propyl group in place of the methyl group on the 2-position of the indole ring. In conjunction with vacuolization of late endosomal compartments, MOIIPP partially impairs lysosome-directed trafficking of cell surface receptors and procathepsins [26]. However, the effects of MOIIPP on exosome secretion have not yet been explored.

Another intriguing molecule is vacuolin-1, an unrelated triazine-based compound that was initially characterized by Feng et al. [27]. Like MOIIPP, it induces vacuolization of late endosomal and lysosomal compartments without affecting cell viability [28]. Vacuolin-1 has been reported to inhibit fusion of endosomes and autophagosomes with lysosomes [29] and to impair Ca<sup>2+</sup>-dependent exocytosis of lysosomes [28], while having no effect on trafficking of vesicular structures termed ‘enlargeosomes’ to the plasma membrane [28]. In the present study we utilized cultured human glioblastoma cells and 293T cells to assess the effects of MOIIPP and vacuolin-1 on exosome production. The results suggest that both compounds may have potential utility as non-toxic agents to enhance the cellular release of exosomes.

## Materials and methods

### Cell culture

U251 human glioblastoma cells were purchased from the DCT Tumor Repository (National Cancer Institute,

Frederick, MD). Human embryonal kidney 293T cells were obtained from the American Type Culture Collection, Manassas, VA. Stock cultures of both cell lines were maintained in Dulbecco’s modified Eagle medium (DMEM) containing 10% (v/v) fetal bovine serum (FBS) (JR Scientific, Woodland, CA) at 37 °C with an atmosphere of 5% CO<sub>2</sub> in air. Cultures were passaged for less than 6 months and were monitored periodically for mycoplasma contamination.

### Isolation of exosomes

Cells were seeded in 10 cm diameter culture dishes at 500,000 cells/dish and maintained for 24 h in DMEM supplemented with 10% Gibco™ exosome-depleted FBS (Thermo Fisher Scientific, Waltham, MA). The medium was then replaced with fresh medium containing either 10 μM MOIIPP, synthesized as described [24] or 1 μM vacuolin-1 (Santa Cruz Biotechnology, Santa Cruz, CA) dissolved in DMSO. Control cultures contain an equivalent volume of the DMSO vehicle (0.1%) in the medium. After 24 h, the medium was collected from the dishes (typically 10–12 dishes per condition) and the attached cells were pooled and counted with a Coulter Counter, model Z1 (Beckman-Coulter, Indianapolis, IN). Exosomes were isolated from medium using the Exo-spin™ Exosome Purification system (Cell Guidance Systems, St. Louis, MO). The medium was pre-cleared by centrifugation at 4 °C, first at 300×*g* for 10 min and then at 16,000×*g* for 30 min. Then a volume of Buffer A equal to half the volume of medium was added and the mixture was incubated overnight at 4 °C. The precipitate, enriched with exosomes, was collected by centrifugation at 16,000×*g* for 1 h, and the pellet was re-suspended in 100 μl of Dulbecco’s phosphate-buffered saline (PBS), pH 7.4. The material was applied to an Exo-Spin column equilibrated with PBS, and the purified exosomes were eluted in 200 μl of PBS.

### Electron microscopy

Aliquots of purified exosomes obtained from control and drug-treated cell cultures were fixed with 4% paraformaldehyde and stained with 2% uranyl acetate on Formvar carbon-coated electron microscopy grids. Vesicles were visualized using a Hitachi HD-2300 transmission electron microscope at an accelerating voltage of 200 kV. Electron microscopy of vacuolated cells was carried out as described previously [30].

### Dynamic light scattering (DLS)

Exosomes suspended in PBS were subjected to DLS using a Nicomp 380 ZLS instrument (Particle Sizing Systems,

Port Richey, FL). Samples were placed in the path of a helium neon laser of wavelength 658 nm at 23 °C, and data were collected at a scattering angle of 90°. For each sample, three measurements of 8 min each were performed, and the particle size distribution (number-weighted diameter) was displayed.

### Immunoblot analysis

The cells in the dishes used for collection of exosomes were washed three times with PBS and lysed in SDS sample buffer [31]. The protein concentration was determined by colorimetric assay using Bio-Rad reagent (Bio-Rad, Richmond, CA). Samples containing equal amounts of total cell protein were subjected to SDS-PAGE and immunoblot analysis using procedures described previously [32]. For analysis of proteins in exosomes, equal volumes of purified exosomes isolated from control or treated cells were mixed with 1/5 volume of 5X SDS sample buffer prior to SDS-PAGE. Monoclonal antibodies against CD63 (H5C6) and LAMP-1 (H4A3) were obtained from the Developmental Studies Hybridoma Bank (Iowa City, IA). Antibodies against Alix (sc-53540) and cytochrome c (sc-13560) were from Santa Cruz Biotechnology (Santa Cruz, CA), and the antibody against lamin B<sub>2</sub> (12255) was from Cell Signaling Technology (Danvers, MA). Incubations with primary antibodies were carried out overnight at 4 °C at the following dilutions: 1:500 for CD63 and LAMP-1; 1:1000 for Alix, cytochrome c, and lamin B<sub>2</sub>. HRP-coupled goat anti-mouse IgG (cat. no. 554002) and goat anti-rabbit IgG (cat. no. 554001) were obtained from BD Biosciences (San Jose, CA). Secondary antibodies were diluted 1:2000 and incubated with the blots for 1 h. Chemiluminescent signals were quantified using an Alpha Innotech FluorChem HD2 imaging system with Alpha View software (San Jose, CA).

### Analysis of miRNAs

Total RNA was extracted and purified from cultured cells or exosomes using QIAzol lysis reagent followed by RNeasy Mini spin-columns, according to the manufacturer's protocol (SA Biosciences/Qiagen, Germantown, MD). cDNA was generated by reverse transcription of 150 ng of total RNA, using the miScript II RT kit (Qiagen). RNA and cDNA were quantified and checked for purity (OD 260/280) using a Nano-Drop-1000 spectrophotometer (Thermo Fisher). For initial profiling of the miRNAs expressed in control or MOPIPP-treated cells, equal amounts of cDNA were applied to Human Brain Cancer miScript<sup>®</sup> miRNA PCR arrays (MIHS-108Z) (SA Biosciences/Qiagen), and real-time PCR reactions were carried

in an Applied Biosystems StepOne Plus<sup>™</sup> system using SYBR Green master mix. Ct values for the individual miRNAs were normalized to the average Ct value for six snoRNA/snRNA miScript PCR controls included on each array, yielding  $\Delta$ Ct values. For comparisons of the miRNA contents of exosomes collected from the medium of cells treated with MOPIPP, vacuolin-1, or vehicle (DMSO), individual miScript primers were purchased for six of the most highly expressed miRNAs detected in U251 cells (SA Biosciences/Qiagen). The primers were reconstituted in SYBR green master mix and combined with cDNAs derived from equal amounts of exosomal RNA (150 ng). RT-PCR reactions were carried out in triplicate to obtain Ct values for each miRNA. The Ct values were normalized to the average Ct value for an endogenous "housekeeping" miRNA, SNORD68, in the same exosome cDNA samples to obtain  $\Delta$ Ct values.

## Results

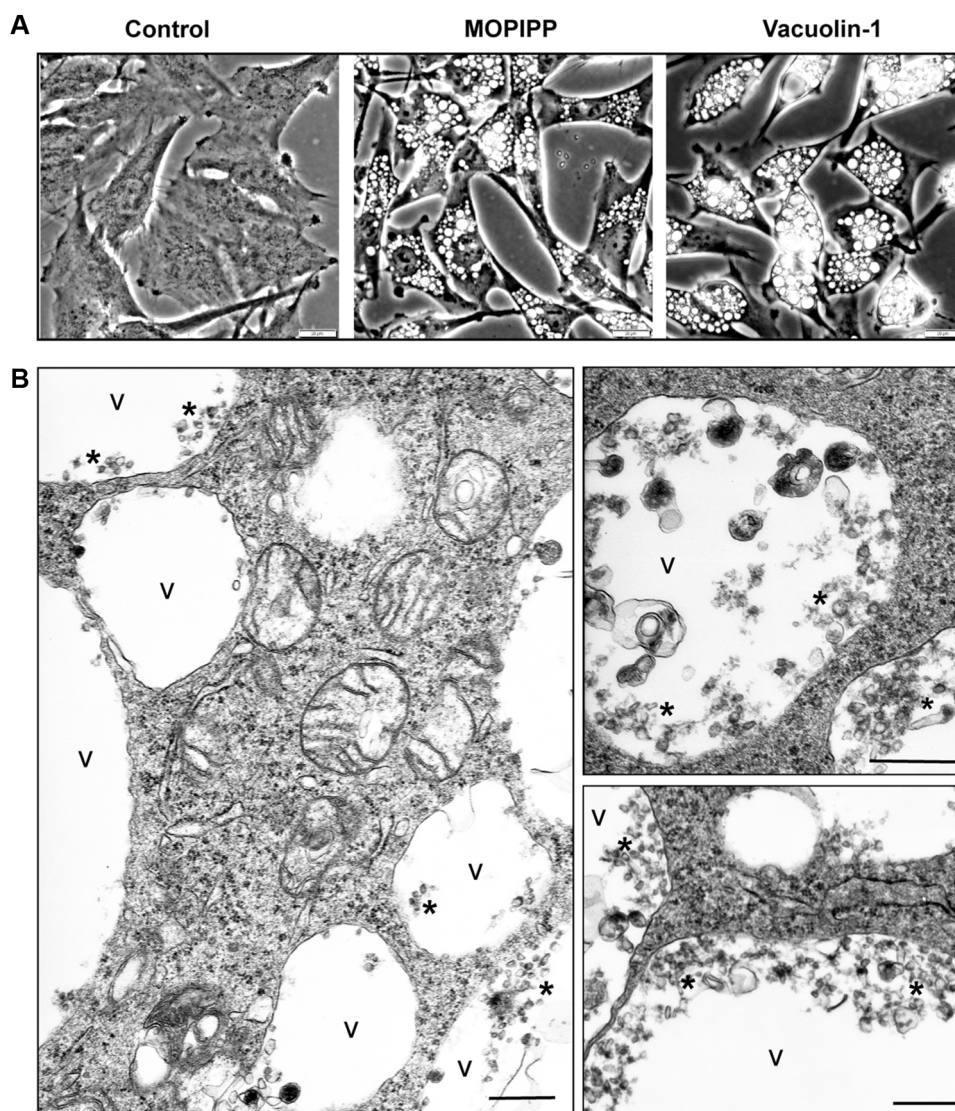
### Characterization of exosomes

In accord with previous reports [24, 26], treatment of cultured U251 glioblastoma cells with MOPIPP resulted in vacuolization of endocytic compartments. The accumulation of numerous vacuoles was readily detected by phase contrast microscopy (Fig. 1a). Treatment with vacuolin-1 induced a very similar phenotype (Fig. 1a). Despite the extreme vacuolization, the cells treated with both compounds remained attached to the culture dishes and continued to proliferate. Electron microscopy revealed that most of the vacuoles in the cells treated with MOPIPP were surrounded by a single membrane and were largely devoid of intraluminal contents (Fig. 1b). However, a distinct subpopulation of vacuoles (approximately 20–30%) contained clusters of heterogeneous vesicles, many of which were of a size (<50 nm) consistent with ILVs and exosomes (examples shown in Fig. 1b).

When 24h conditioned media were collected from control and drug-treated cultures and subjected to a procedure designed to yield purified exosomes, electron microscopy showed that the final exosome fraction consisted mainly of vesicles with diameters of approximately 25–30 nm (Fig. 2a), matching the lower end of the size range reported for exosomes. There were no discernable differences in the morphologies of the vesicles obtained from the treated cells compared to the control. Particle analysis by DLS confirmed that the purified vesicle populations had unimodal distributions with mean diameters in the range of 18–27 nm. Differences between control and treated cells were not statistically significant (Fig. 2b).



**Fig. 1** Comparison of cell morphologies in cultures treated with MOIPIP and vacuolin-1. **a** U251 cells were examined by phase contrast microscopy after 24 h treatment with 10  $\mu$ M MOIPIP, 1  $\mu$ M vacuolin-1 or an equivalent volume of DMSO (control). Scale bars 20  $\mu$ m. **b** Electron micrographs of U251 cells after 24 h treatment with MOIPIP show many large vacuoles (v), with some containing clusters of ILVs (asterisks). Scale bars = 500 nm



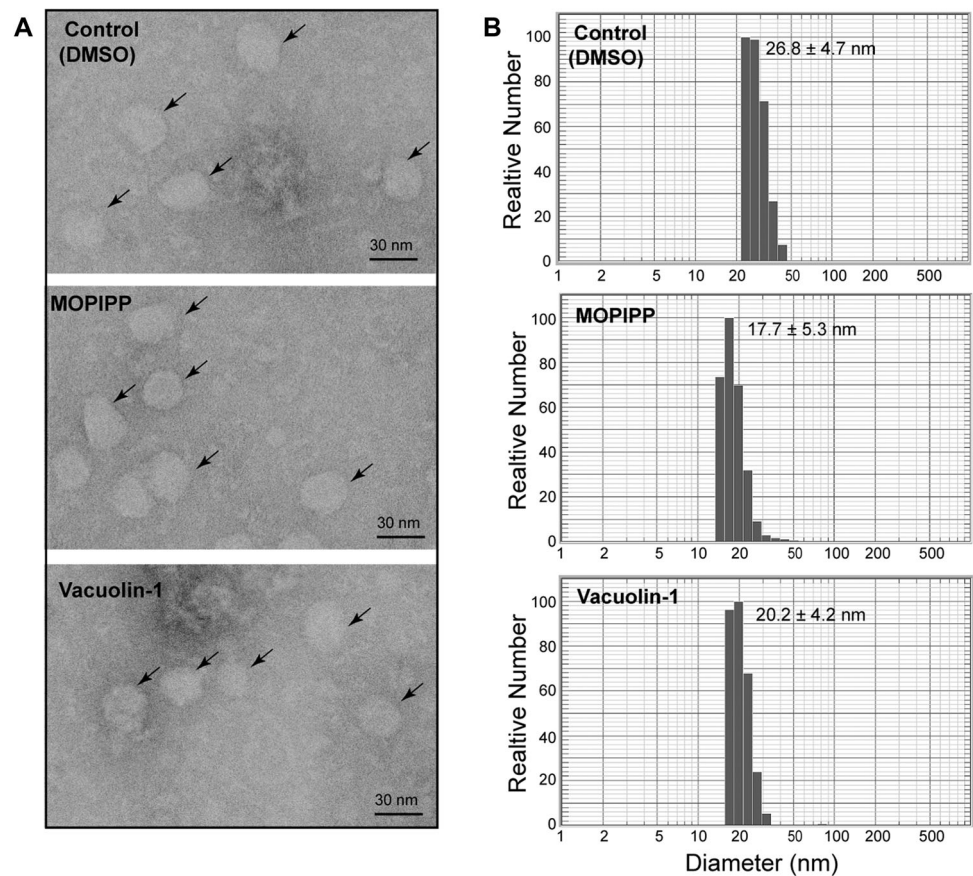
### Quantification of exosome marker proteins

To determine if treatment with MOIPIP and/or vacuolin-1 might alter the production of exosomes, conditioned medium was pooled from 10 to 12 control or treated cultures and exosomes were isolated as described above. The cells from the same cultures were also harvested and pooled. Figure 3a shows that comparable numbers of cells were collected from the control and drug-treated cultures, consistent with the lack of growth inhibition by MOIPIP and vacuolin-1. The immunoblots in Fig. 3b demonstrate that cytochrome c and lamin B<sub>2</sub>, markers for mitochondria and nuclear envelope, respectively, were not detectable in the purified exosome populations, confirming that the latter were not contaminated with intracellular organelles released via cell lysis. In Fig. 3c–e, the isolated exosomes and cells were probed for three proteins commonly enriched in MVEs and exosomes: Alix, a protein involved in the biogenesis of endosomal ILVs

[33]; CD63, a member of tetraspanin protein family [34], and LAMP-1, an abundant membrane glycoprotein in lysosomes and late endosomes [35, 36]. The results show that the relative amounts of all three proteins were increased by several folds in the extracellular vesicle preparations from cultures treated with MOIPIP (Fig. 3c–e). An even greater increase was observed in the cultures treated with vacuolin-1. In contrast, changes in expression of the same marker proteins in the corresponding cell populations were comparatively modest (Fig. 3c–e). Since the exosomes were isolated from nearly identical numbers of cells in the control and treated cultures (Fig. 3a), the results suggest that MOIPIP and vacuolin-1 promote an increase in the release of exosomes into the extracellular environment.

To determine if MOIPIP and vacuolin-1 would have a similar effect in a cell line commonly used for large-scale exosome production, we tested these compounds in 293T cells [37]. Both compounds induced extensive

**Fig. 2** Exosomes isolated from cultures treated with MOIPIP or vacuolin-1 are morphologically similar to exosomes isolated from cells treated with vehicle (DMSO). U251 cells were treated for 24 h with the indicated compounds and exosomes were collected from the medium as described in “Materials and methods.” The exosome preparations were characterized by transmission electron microscopy (a) or DLS (b)



vacuolization of 293T cells (Fig. 4a) without substantially reducing the yield of cells harvested from the treated cultures (Fig. 4b). As in the case of the glioblastoma cells, both MOMIPP and vacuolin-1 caused multi-fold increases in Alix and CD63 in exosome fractions collected from comparable numbers of cells (Fig. 4c, d). At the same time, the intracellular contents of these proteins were unaffected or modestly reduced (Fig. 4c, d).

### Comparison of miRNA profiles

miRNAs carried by exosomes play important roles in inter-cellular communication [5, 6]. Thus, we asked if, in addition to increasing exosome output, MOIPIP and vacuolin-1 might alter the miRNA composition of the exosomes. We began by profiling miRNAs expressed in untreated U251 glioblastoma cells, using a RT-PCR array that detects 84 miRNAs commonly associated with human brain cancers. Based on their  $\Delta C_t$  values relative to a panel of six normalization controls (Fig. 5a), we selected 13 miRNAs with high expression for further comparison between control and MOIPIP-treated cells. As shown in Fig. 5b, treatment with MOIPIP did not cause major changes in the cellular expression of any of the selected miRNAs. Among the miRNAs profiled on the array, we selected six for profiling in

exosomes released from the U251 cells. Triplicate reactions starting with equal amounts of total exosomal RNA were carried out to obtain  $C_t$  values. Although the selection of a definitive RT-PCR standard for normalization of exosomal miRNA is controversial, there is evidence from studies of human serum samples that the endogenous miRNA, SNORD68, can serve as a useful “housekeeping” standard [38]. Therefore SNORD68 was used to obtain  $\Delta C_t$  values for the exosomal miRNAs released from drug-treated and untreated cells (Fig. 5c). Comparison of the miRNAs in exosomes (Fig. 5b) vs cells (Fig. 5c) from the untreated cultures (solid bars) revealed that not all miRNAs are incorporated into exosomes in direct proportion to their intracellular abundance. For example, miR-21-5p was the most abundant in cells, but was the least abundant of the tested group in the exosomes. The miRNA contents of the exosomes released from cells treated with vacuolin-1 were generally similar to the untreated controls. In the MOIPIP-treated cells the exosomal miRNA profile was not grossly altered. However, we did observe small but significant decreases in the  $\Delta C_t$  values for all of the miRNAs in comparison to the untreated controls. Examination of the raw  $C_t$  values for each miRNA (Fig. 5d) suggests that these variations are due mainly to a slightly lower abundance of the miR-SNORD68 standard in the exosomes from the

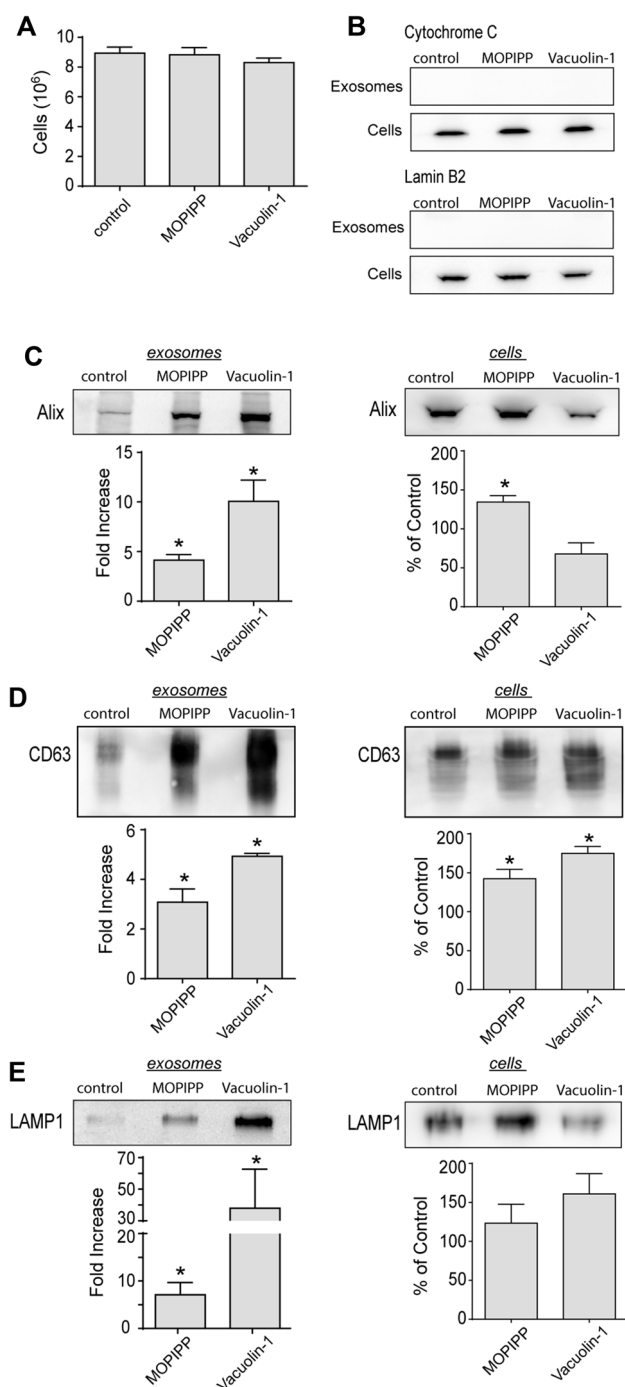


**Fig. 3** MOMIPP and vacuolin-1 increase the amounts of exosomal marker proteins in vesicle fractions recovered from conditioned medium. In three separate experiments, U251 cells were treated for 24 h with 10  $\mu$ M MOMIPP, 1  $\mu$ M vacuolin-1, or an equivalent volume of DMSO vehicle. The cells from each experiment were counted (mean  $\pm$  SEM) (**a**), and the medium from the same cultures was used to prepare exosomes with the Exo-spin<sup>TM</sup> Purification method. Equal aliquots of the final exosome preparations were subjected to western blot analysis for Alix (**c**), CD63 (**d**), and LAMP1 (**e**) (*left panels*). The cells from these experiments were immunoblotted for the same proteins, with equal amounts of protein loaded on each lane (*right panels*). Representative blots are shown. For the exosomes, the fold-increase in the treated cells relative to the DMSO-treated controls is graphed below each blot (mean  $\pm$  SEM). Asterisks denote significant increases ( $p \leq 0.05$ ) relative to paired controls, determined by Student's *t* test. For the cells, the signals for the proteins in the treated cells are expressed as percent of the corresponding controls (mean  $\pm$  SEM), and significant changes ( $p \leq 0.05$ ) are noted with asterisks. The blots in panel (**b**) demonstrate that proteins associated with mitochondria (cytochrome c) or nuclear envelope (lamin B<sub>2</sub>) were not detectable in the exosome fractions

MOMIPP-treated cells, rather than a major effect of the drug on expression or export of the six selected miRNAs.

## Discussion

The results show that vacuolization of late endosomal compartments induced by two distinct small molecules, MOMIPP and vacuolin-1, is accompanied by a several-fold increase in exosomal marker proteins in extracellular vesicles prepared from comparable numbers of glioblastoma cells. Cell proliferation and viability were not markedly impaired by these compounds, and the characteristics of the exosomes from treated cells were similar to the controls. Since the intracellular amounts of the marker proteins were only modestly affected by the compounds, the results are indicative of an increase in exosome biogenesis and/or secretion in cells treated with MOMIPP and vacuolin-1.

Small molecules that promote vacuolization of late endosomal compartments have the potential to affect exosome production in several ways. In one scenario, vacuolization of endosomes could disrupt the molecular machinery for the formation of ILVs, so that any MVEs that subsequently fuse with the plasma membrane release



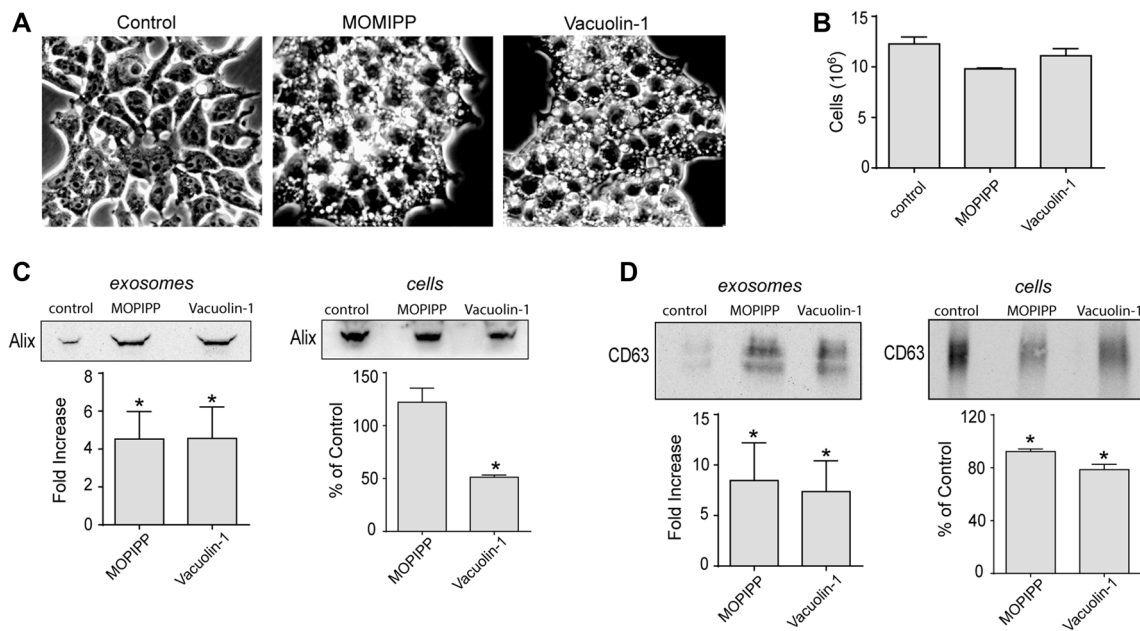


**Fig. 4** MOIPIP and vacuolin-1 increase the amounts of exosomal marker proteins in vesicle fractions recovered from 293T cells. In three separate experiments, 293T cells were treated for 24 h with 10  $\mu$ M MOIPIP, 1  $\mu$ M vacuolin-1, or an equivalent volume of DMSO vehicle. The cells from each experiment were examined by phase contrast microscopy (a) then pooled and counted (mean  $\pm$  SEM) (b). The conditioned medium from the same cultures was used to prepare exosomes with the Exo-spin<sup>TM</sup> Purification method. Equal aliquots of the final exosome preparations were subjected to western blot analysis for Alix (c) and CD63 (d) (left panels). The cells from

these experiments were immunoblotted for the same proteins, with equal amounts of protein loaded on each lane (right panels). Representative blots are shown. For the exosomes, the fold-increase in the treated cells relative to the DMSO-treated controls is graphed below each blot (mean  $\pm$  SEM). Asterisks denote significant increases ( $p \leq 0.05$ ) relative to paired controls, determined by Student's *t* test. For the cells, the signals for the proteins in the treated cells are expressed as percent of the corresponding controls (mean  $\pm$  SEM), and significant changes ( $p \leq 0.05$ ) relative to the controls are noted with asterisks

fewer exosomes. In a second model, formation of ILVs might remain unaffected, but trafficking of enlarged MVEs to the cell surface might be disrupted, also resulting in diminished exosome secretion. Finally, in a third model, one might envision that drug-induced vacuoles derived from late endosomes could retain the ability to generate ILVs, but be unable to merge with lysosomes where the vesicles are degraded. In that case, enlarged MVEs might accumulate and deliver more ILVs to the extracellular environment, provided that they remain competent to fuse with the plasma membrane. The latter model seems most likely to explain the apparent increase in exosome secretion (Fig. 3c–e), considering that many vacuoles in MOIPIP-treated cells contained numerous ILVs (Fig. 1b), and previous reports have demonstrated defective endosome  $\rightarrow$  lysosome trafficking in cells treated with MOIPIP [26] and vacuolin-1 [29]. Confirmation of this model will require further studies to determine if ILV biogenesis and trafficking of vacuolated MVEs to the plasma membrane remain intact in cells treated with the vacuole-inducing agents.

The miRNA cargo carried by exosomes may differ from the miRNA profile of the producer cell, implying that incorporation of miRNAs into exosomes is not random [39]. Details about the sorting complexes that interact with MVEs and govern the loading of miRNAs into exosomes have begun to emerge [40–42]. Herein we found that extensive vacuolization of endosomal compartments did not affect the overall expression of several common miRNAs in glioblastoma cells (Fig. 5b). Several of the most highly expressed cellular miRNAs were represented in the exosome populations. However, their relative abundance in the exosomes did not always reflect their abundance in the cells (e.g., compare miR-21-5p in Fig. 5b vs Fig. 5c). This is consistent with the aforementioned concept of selective sorting of some miRNAs into exosomes. Comparison of the miRNA compositions in exosomes collected from treated versus untreated cells (Fig. 5c, d) suggests that although some variations occur, particularly in cells treated with MOIPIP, overall the vacuole-inducing compounds do not radically alter the relative concentrations of most of the miRNAs. Thus, while the analysis of exosomal proteins

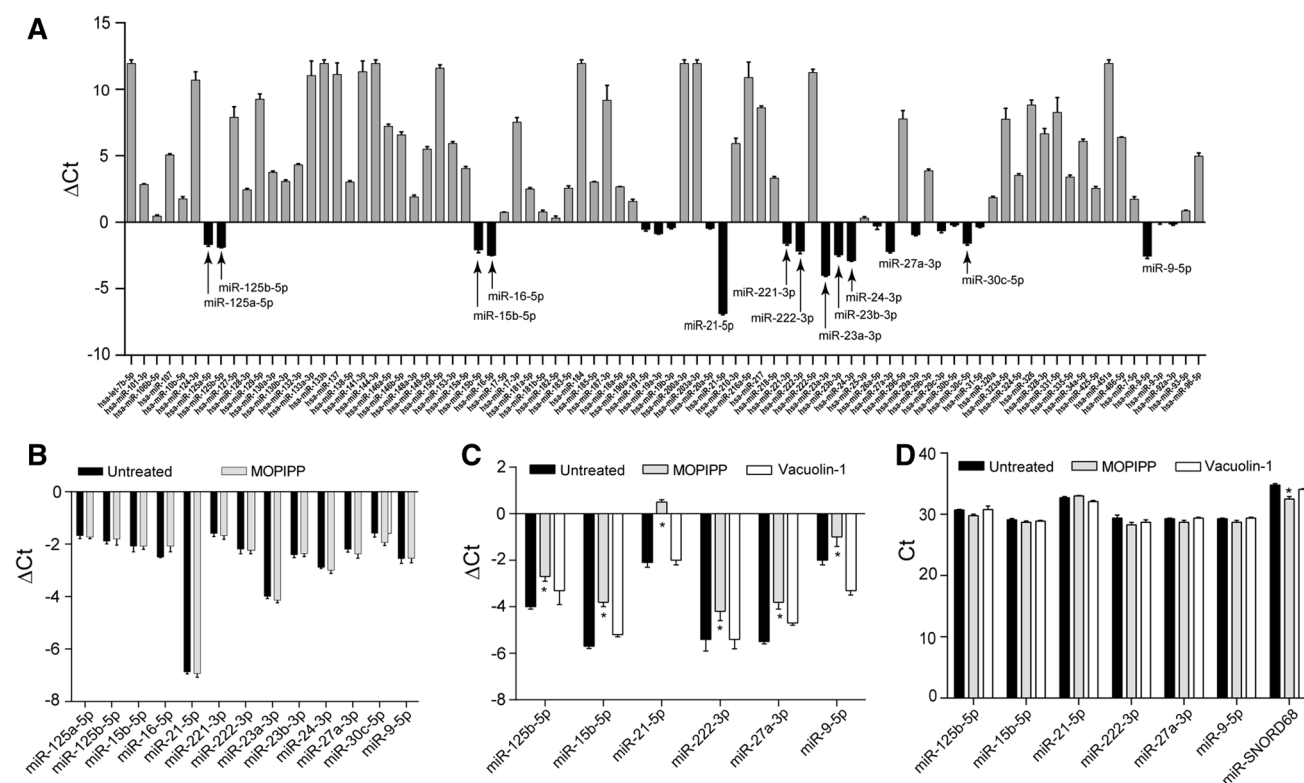


**Fig. 5** MOPIPP and vacuolin-1 do not have major effects on the profile of miRNAs represented in exosomes. **a** Cellular miRNAs expressed in untreated U251 cells were profiled using the Human Brain Cancer miScript<sup>®</sup> arrays ( $n = 3$ ) and  $\Delta$ Ct values were determined using the six snoRNA/snRNA miScript PCR controls included on each array. The specific miRNAs selected for further study are indicated with arrows. **b** U251 cells were treated with 10  $\mu$ M MOPIPP or an equivalent volume of DMSO for 24 h and cellular

expression of each of the indicated miRNAs was determined by RT-PCR ( $n = 3$ ). **c, d** Exosomes were isolated from U251 cells treated with MOPIPP, vacuolin-1, or DMSO and equal amounts of exosomal RNA were subjected to reverse transcription and RT-PCR in triplicate to quantify the indicated miRNAs. The results were normalized to miR-SNORD68 to obtain  $\Delta$ Ct (**c**) or depicted as raw Ct values (**d**). The values marked with asterisks in the MOPIPP-treated cells were significantly different from the controls at  $p \leq 0.05$

indicates that MOPIPP and vacuolin-1 induce large increases in exosome secretion, the exosomes appear to be qualitatively similar to those collected from untreated cells in terms of their miRNA cargo.

Among the possible therapeutic applications of exosomes, considerable attention has been devoted to using these vesicles as nanocarriers for packaging and delivery of small molecules (e.g., anti-cancer drugs), miRNAs, and proteins [8, 9]. As new methods are developed to engineer exosome cargoes in producer cells, one of the major impediments to more widespread development of exosome-based therapies is the low yield of exosomes. Our finding that the effects of MOPIPP and vacuolin-1 on exosome production in glioblastoma cells also extend to the commonly used 293T cell line suggests that these small molecules may have potential general utility as non-cytotoxic pharmacological agents to boost exosome production for biotechnology and therapeutic purposes. In this regard, further investigation of mechanism of action of these compounds is warranted.

**Acknowledgements** We thank Christopher J. Trabbic and Paul W. Erhardt for supplying MOPIPP, and William T. Gunning III for assistance with electron microscopy of cells. This work was supported by NIH Grant R01 CA115495 and by the Harold and Helen McMaster Endowment for Biochemistry and Molecular Biology.

## References

- Vlassov AV, Magdaleno S, Setterquist R, Conrad R (2012) Exosomes: current knowledge of their composition, biological functions, and diagnostic and therapeutic potentials. *Biochim Biophys Acta* 1820(7):940–948
- Andaloussi EL, Mager I, Breakefield XO, Wood MJ (2013) Extracellular vesicles: biology and emerging therapeutic opportunities. *Nat Rev Drug Discov* 12(5):347–357
- Hu G, Drescher KM, Chen XM (2012) Exosomal miRNAs: biological properties and therapeutic potential. *Front Genet* 3:56
- Thind A, Wilson C (2016) Exosomal miRNAs as cancer biomarkers and therapeutic targets. *J Extracell Vesicles* 5:31292
- Simons M, Raposo G (2009) Exosomes—vesicular carriers for intercellular communication. *Curr Opin Cell Biol* 21(4):575–581
- Mathivanan S, Ji H, Simpson RJ (2010) Exosomes: extracellular organelles important in intercellular communication. *J Proteomics* 73(10):1907–1920



7. Azmi AS, Bao B, Sarkar FH (2013) Exosomes in cancer development, metastasis, and drug resistance: a comprehensive review. *Cancer Metastasis Rev* 32(3–4):623–642
8. Johnsen KB, Gudbergsson JM, Skov MN, Pilgaard L, Moos T, Duroux M (2014) A comprehensive overview of exosomes as drug delivery vehicles—endogenous nanocarriers for targeted cancer therapy. *Biochim Biophys Acta* 1846(1):75–87
9. Ha D, Yang N, Nadithe V (2016) Exosomes as therapeutic drug carriers and delivery vehicles across biological membranes: current perspectives and future challenges. *Acta Pharm Sin B* 6(4):287–296
10. Fevrier B, Raposo G (2004) Exosomes: endosomal-derived vesicles shipping extracellular messages. *Curr Opin Cell Biol* 16(4):415–421
11. Harding CV, Heuser JE, Stahl PD (2013) Exosomes: looking back three decades and into the future. *J Cell Biol* 200(4):367–371
12. Stahl PD, Barbieri MA (2002) Multivesicular bodies and multivesicular endosomes: the “ins and outs” of endosomal traffic. *SciSTKE* 141:E32
13. Piper RC, Katzmann DJ (2007) Biogenesis and function of multivesicular bodies. *Annu Rev Cell Dev Biol* 23:519–547
14. Raposo G, Stoorvogel W (2013) Extracellular vesicles: exosomes, microvesicles, and friends. *J Cell Biol* 200(4):373–383
15. Trajkovic K, Hsu C, Chiantia S, Rajendran L, Wenzel D, Wieland F, Schwille P, Brugger B, Simons M (2008) Ceramide triggers budding of exosome vesicles into multivesicular endosomes. *Science* 319(5867):1244–1247
16. Savina A, Furlan M, Vidal M, Colombo MI (2003) Exosome release is regulated by a calcium-dependent mechanism in K562 cells. *J Biol Chem* 278(22):20083–20090
17. Parolini I, Federici C, Raggi C, Lugini L, Palleschi S, De Milito A, Coscia C, Iessi E, Logozzi M, Molinari A, Colone M, Tatti M, Sargiacomo M, Fais S (2009) Microenvironmental pH is a key factor for exosome traffic in tumor cells. *J Biol Chem* 284(49):34211–34222
18. Ostrowski M, Carmo NB, Krumeich S, Fanget I, Raposo G, Savina A, Moita CF, Schauer K, Hume AN, Freitas RP, Goud B, Benaroch P, Hacohen N, Fukuda M, Desnos C, Seabra MC, Darchen F, Amigorena S, Moita LF, Thery C (2010) Rab27a and Rab27b control different steps of the exosome secretion pathway. *Nat Cell Biol* 12(1):19–30
19. Hsu C, Morohashi Y, Yoshimura S, Manrique-Hoyos N, Jung S, Lauterbach MA, Bakhti M, Gronborg M, Mobius W, Rhee J, Barr FA, Simons M (2010) Regulation of exosome secretion by Rab35 and its GTPase-activating proteins TBC1D10A-C. *J Cell Biol* 189(2):223–232
20. Savina A, Vidal M, Colombo MI (2002) The exosome pathway in K562 cells is regulated by Rab11. *J Cell Sci* 115(Pt 12):2505–2515
21. Aki T, Nara A, Uemura K (2012) Cytoplasmic vacuolization during exposure to drugs and other substances. *Cell Biol Toxicol* 28(3):125–131
22. Maltese WA, Overmeyer JH (2014) Methuosis: nonapoptotic cell death associated with vacuolization of macropinosome and endosome compartments. *Am J Pathol* 184(6):1630–1642
23. Robinson MW, Overmeyer JH, Young AM, Erhardt PW, Maltese WA (2012) Synthesis and evaluation of indole-based chalcones as inducers of methuosis, a novel type of nonapoptotic cell death. *J Med Chem* 55(5):1940–1956
24. Trabbic CJ, Dietsch HM, Alexander EM, Nagy PI, Robinson MW, Overmeyer JH, Maltese WA, Erhardt PW (2014) Differential induction of cytoplasmic vacuolization and methuosis by novel 2-indolyl-substituted pyridinylpropenones. *ACS Med Chem Lett* 5(1):73–77
25. Trabbic CJ, Overmeyer JH, Alexander EM, Crissman EJ, Kvale HM, Smith MA, Erhardt PW, Maltese WA (2015) Synthesis and biological evaluation of indolyl-pyridinyl-propenones having either methuosis or microtubule disruption activity. *J Med Chem* 58(5):2489–2512
26. Mbah NE, Overmeyer JH, Maltese WA (2017) Disruption of endolysosomal trafficking pathways in glioma cells by methuosis-inducing indole-based chalcones. *Cell Biol Toxicol* 33:263–281
27. Feng Y, Yu S, Lasell TK, Jadhav AP, Macia E, Chardin P, Melancon P, Roth M, Mitchison T, Kirchhausen T (2003) Exo1: a new chemical inhibitor of the exocytic pathway. *Proc Natl Acad Sci USA* 100(11):6469–6474
28. Cerny J, Feng Y, Yu A, Miyake K, Borgonovo B, Klumperman J, Meldolesi J, McNeil PL, Kirchhausen T (2004) The small chemical vacuolin-1 inhibits Ca<sup>2+</sup>-dependent lysosomal exocytosis but not cell resealing. *EMBO Rep* 5(9):883–888
29. Lu Y, Dong S, Hao B, Li C, Zhu K, Guo W, Wang Q, Cheung KH, Wong CW, Wu WT, Markus H, Yue J (2014) Vacuolin-1 potently and reversibly inhibits autophagosome-lysosome fusion by activating RAB5A. *Autophagy* 10(11):1895–1905
30. Johnson EE, Overmeyer JH, Gunning WT, Maltese WA (2006) Gene silencing reveals a specific function of hVps34 phosphatidylinositol 3-kinase in late versus early endosomes. *J Cell Sci* 119(Pt 7):1219–1232
31. Laemmli UK (1970) Cleavage of structural proteins during the assembly of the head of bacteriophage T4. *Nature* 227:680–685
32. Maltese WA, Wilson S, Tan Y, Suomensaari S, Sinha S, Barbour R, McConlogue L (2001) Retention of the Alzheimer’s amyloid precursor fragment C99 in the endoplasmic reticulum prevents formation of amyloid beta-peptide. *J Biol Chem* 276(23):20267–20279
33. Bissig C, Gruenberg J (2014) ALIX and the multivesicular endosome: ALIX in Wonderland. *Trends Cell Biol* 24(1):19–25
34. Zoller M (2009) Tetraspanins: push and pull in suppressing and promoting metastasis. *Nat Rev Cancer* 9(1):40–55
35. Logozzi M, De Milito A, Lugini L, Borghi M, Calabro L, Spada M, Perdicchio M, Marino ML, Federici C, Iessi E, Brambilla D, Venturi G, Lozupone F, Santinami M, Huber V, Maio M, Rivoltini L, Fais S (2009) High levels of exosomes expressing CD63 and caveolin-1 in plasma of melanoma patients. *PLoS ONE* 4(4):e5219
36. Sheldon H, Heikamp E, Turley H, Dragovic R, Thomas P, Oon CE, Leek R, Edelman M, Kessler B, Sainson RC, Sargent I, Li JL, Harris AL (2010) New mechanism for Notch signaling to endothelium at a distance by Delta-like 4 incorporation into exosomes. *Blood* 116(13):2385–2394
37. Li J, Chen X, Yi J, Liu Y, Li D, Wang J, Hou D, Jiang X, Zhang J, Wang J, Zen K, Yang F, Zhang CY, Zhang Y (2016) Identification and characterization of 293T cell-derived exosomes by profiling the protein, mRNA and microRNA components. *PLoS ONE* 11(9):e0163043
38. Abd-El-Fattah AA, Sadik NA, Shaker OG, Aboulftouh ML (2013) Differential microRNAs expression in serum of patients with lung cancer, pulmonary tuberculosis, and pneumonia. *Cell Biochem Biophys* 67(3):875–884
39. Zhang J, Li S, Li L, Li M, Guo C, Yao J, Mi S (2015) Exosome and exosomal microRNA: trafficking, sorting, and function. *Genomics Proteomics Bioinform* 13(1):17–24
40. Janas T, Janas MM, Sapon K, Janas T (2015) Mechanisms of RNA loading into exosomes. *FEBS Lett* 589(13):1391–1398
41. Shurtleff MJ, Temoche-Diaz MM, Karfilis KV, Ri S, Schekman R (2016) Y-box protein 1 is required to sort microRNAs into exosomes in cells and in a cell-free reaction. *eLife*. doi:10.7554/eLife.19276
42. Santangelo L, Giurato G, Cicchini C, Montaldo C, Mancone C, Tarallo R, Battistelli C, Alonzi T, Weisz A, Tripodi M (2016) The RNA-binding protein SYNCRIP is a component of the hepatocyte exosomal machinery controlling microRNA sorting. *Cell Rep* 17(3):799–808